1 **Projected increases in wildfires may challenge regulatory curtailment of PM$_{2.5}$ over the**

2 **eastern US by 2050**

4 Chandan Sarangi[1,2]*, Yun Qian[2]*, L. Ruby Leung[2], Yang Zhang[3], Yufei Zou[4,2], Yuhang

5 Wang[4]

7 [1] Indian Institute of Technology Madras, Chennai, India

8 [2] Pacific Northwest National Laboratory, Richland, WA, USA

9 [3] Department of Civil and Environmental Engineering, Northeastern University, Boston, MA

10 [4] School of Earth and Atmospheric Sciences, Georgia Institute of Technology, Atlanta, GA,

11 USA.

14 *Corresponding Authors:

15 chandansarangi@iitm.ac.in

16 yun.qian@pnnl.gov

21 **Abstract**

22 Anthropogenic contribution to the overall fine particulate matter ($PM_{2.5}$) concentrations has

23 been declining sharply in North America. In contrast, a steep rise in wildfire-induced air

24 pollution events with recent warming is evident in the region. Here, based on coupled fire-

25 climate-ecosystem model simulations, summertime wildfire-induced $PM_{2.5}$ concentrations are

26 projected to nearly double in North America by the mid-21st century compared to the

27 present. More strikingly, the projected enhancement in fire-induced $PM_{2.5}$ (~ 1-2 $\mu g/m^3$) and

28 its contribution (~15-20%) to the total $PM_{2.5}$ are distinctively significant in the eastern US.

29 This can be attributed to downwind transport of smoke from future enhancement of wildfires

30 in North America to the eastern US and associated positive climatic feedback on $PM_{2.5}$ i.e.

31 perturbations in circulation, atmospheric stability and precipitation. Therefore, the anticipated

32 reductions in $PM_{2.5}$ from regulatory controls on anthropogenic emissions could be

33 significantly compromised in the future in the densely populated eastern US.

34 **Key points:**

35   1) Wildfire-$PM_{2.5}$ associations studied based on unprecedented two-way coupled fire-

36   climate-ecosystem model simulations

37   2) A steep rise in wildfire-induced air pollution events with recent warming is evident in

38   the region

39   3) The transported smoke from enhanced wildfires in North America can severely affect

40   air quality over Eastern US

41

42 **Keywords:** wildfire emissions, climate change, air quality, smoke transport, wildfire-climate-

43 ecosystem interactions

1. **Introduction**

Wildfires are widespread burning events in forests, shrub lands, and grazing lands. In North America (mainly Canada and the US), particulate matter emissions from wildfires are a significant source of regional air pollution (Shi et al., 2019; McClure and Jaffe, 2018; Van Der Werf et al., 2010; Jaffe et al., 2008). Since the 1980s, the number of large wildfires and the length of wildfire season have been increasing, and the trends are projected to continue in the future over the western US, Alaska and Canada (Kitzberger et al., 2017; Kirchmeier-Young et al., 2017; Abatzoglou and Williams, 2016; Partain et al., 2016; Jolly et al., 2015; Westerling et al., 2006; Gillett et al., 2004). Accordingly, particulate emissions from wildfires are also anticipated to increase in North America in the 21st century (Knorr et al., 2017; Liu et al., 2016; Val Martin et al., 2015). Human exposure to high concentrations of wildfire-emitted airborne particulate matter of diameter ≤ 2.5 µm ($PM_{2.5}$) is known to have substantial adverse effects on pulmonary and cardiovascular functioning (Anjali et al., 2019; Black et al., 2017), which contribute significantly to global and regional all-cause mortality (Zhang et al., 2020; Hong et al., 2019; Yang et al., 2019; Ford et al., 2018; Johnston. et al., 2012). Therefore, a better understanding of the future changes in wildfire-induced $PM_{2.5}$ and its contribution to the total surface $PM_{2.5}$ is essential.

In the last two decades, ambient air quality in the US has substantially improved due to a decline in $PM_{2.5}$ by ~ 40 % (US EPA, 2018). The decrease in $PM_{2.5}$ is primarily due to curtailment of anthropogenic emissions resulting from US-based efforts to meet regulations such as the Clean Air Act (US EPA, 2009), Cross-State Air Pollution Rule, Regional Haze Rule, and the motor vehicles emissions standards. Consequently, air quality over the contiguous US (CONUS) and Canada has improved steadily such that it is predicted to achieve the targeted National Ambient Air Quality Standards in the future (Nolte et al.,

68   2018). Under this promising scenario, the influence of wildfire-emissions on the total $PM_{2.5}$

69   becomes even more crucial. Depending on the competition between climate-induced increase

70   in wildfires and the regulatory control on anthropogenic emissions, future enhancement in

71   wildfire-induced $PM_{2.5}$ may compromise the reduction in anthropogenic $PM_{2.5}$ concentrations

72   in certain regions. In agreement, recent studies have highlighted the potential for future

73   enhancement in wildfire-induced pollution to diminish the reducing trend in $PM_{2.5}$, primarily

74   over the western US (O'Dell et al., 2019; Ford et al., 2018; Val Martin et al., 2015; Yue et al.,

75   2013).

76   While the fractional wildfire burnt area and fire intensities are the greatest over the

77   western US and Canadian regions within North America, anthropogenic emissions dominate

78   the ambient $PM_{2.5}$ concentration over the eastern US. The inherent geographical separation

79   between the regions with large wildfire emissions and anthropogenic emissions leads to a

80   pertinent question: will future enhancement in wildfires over the western US and Canada

81   have significant effects on $PM_{2.5}$ over the eastern US? Addressing this question is crucial

82   because the declining trend in $PM_{2.5}$ over the eastern US is the major contributor to the

83   observed 40% decrease in $PM_{2.5}$ over the US in the last two decades (US EPA, 2018).

84   Eastward advection of wildfire smoke from Canada and the western US has been found to

85   severely hamper the surface air quality of the central and eastern US under the influence of

86   the prevailing westerlies during the summer months (Brey et al., 2018; Wu et al., 2018;

87   Gunsch et al., 2018; Kaulfus et al., 2017; Dempsey, 2013). The transported wildfire smoke

88   can influence the meteorology and climate via the radiative impact of carbonaceous

89   emissions, changes in land albedo and cloud system perturbations (Ward et al., 2012; Liu et

90   al., 2014). These fire-weather interactions can have positive feedback on the locally-emitted

91   $PM_{2.5}$ in the eastern US by surface cooling and boundary layer suppression(Guan et al.,

92   2020). At the same time, fire-triggered ecosystem changes can induce negative feedback on

93   PM2.5 by reducing the future wildfires over North America (Zou et al., 2020). Thus, two-

94   way interactions between fires and climate that are important for predicting future changes in

95   wildfire locations, intensities, and durations (Harris et al., 2016) as well as associated

96   particulate emissions is essential. However, past studies have mostly employed simple

97   statistical models based on statistical regressions of present-day fire burnt area on the

98   meteorological fields (Liu et al., 2016; Spracklen et al., 2009; Yue et al., 2013; Val Martin et

99   al., 2015), and more recently, one-way coupled modelling (Ford et al., 2018; O'Dell et al.,

100   2019).

101   Here, based on new two-way coupled fire-climate-ecosystem simulations, we

102   demonstrate the significance of wildfire-induced contributions to ambient $PM_{2.5}$ over the

103   eastern US due to enhanced wildfire smoke transportation and smoke-induced changes in

104   weather in eastern US. This enhancement in wildfire-induced $PM_{2.5}$ may potentially challenge

105   the targeted policy-driven reduction of $PM_{2.5}$ in the eastern US. Next, our model setup,

106   experiments and methodology are explained in Section 2, followed by results and discussion

107   in Section 3. The study is summarized in Section 4.

108   **2. Materials and Methods**

109   **2.1. RESFire-CESM Model description**

110   We employ the open-source REgion-Specific ecosystem feedback fire (RESFire)

111   model coupled with the Community Land Model version 4.5 and the Community

112   Atmosphere Model version 5 (CAM5) of the Community Earth System Model (CESM)

113   version 1 (Zou et al., 2019; Neale et al., 2013) to perform two-way coupled simulations.

114   RESFire provides state-of-the-art capabilities to simulate the complex fire-climate-ecosystem

115   interactions globally for fires occurring over wildland, cropland, and peatland. Although

116   wildfires dominate in the North American region, RESFire simulates both wildfires and

117   prescribed fires. Moreover, this integrated setup includes climatic feedback from fire-induced

118   aerosol direct and indirect radiative effects and associated weather changes. It also includes

119   feedback from fire-induced vegetation distribution changes and associated biophysical

120   processes such as evapotranspiration and surface albedo. Sofiev et al. (2012) described the

121   fire plume rise parameterization. Other features in CLM4.5 and CAM5, such as the

122   photosynthesis scheme (Sun et al., 2012), the MAM3 aerosol module (Liu et al., 2012), and

123   the cloud macrophysics scheme (Park et al., 2014), allow for more comprehensive

124   assessments of the climate effects of fires through their interactions with vegetation and

125   clouds. Fire-ecosystem interactions are modelled by simulating fire-induced vegetation

126   mortality and regrowth (and associated land cover change) in RESFire. This approach has

127   been introduced in Zou et al. (2019) and the simulated ecological and climatic effects of

128   wildfires have been evaluated in two sets of sensitivity experiments in Zou et al. (2020).

129   Although fire-climate-ecosystem interactions are considered in this study, our focus is on the

130   fire-induced changes in $PM_{2.5}$ over Canada and the US, so the two vegetation-focused

131   sensitivity experiments reported in Zou et al. (2020) are not included in this paper. Please

132   refer to Zou et al. (2019) and Zou et al. (2020) for more details about the simulation of fire-

133   ecosystem interactions.

134   **2.2 Numerical Experiment and Methodology**

135   We designed two sets of simulations for the present day and future scenarios to

136   quantify the impacts of fire-climate-ecosystem interactions (Table 1). The spatial resolution is

137   0.9° (lat) × 1.25° (lon) with a time step of 30 min. In each set of simulations, we conducted a

138   default all emission included control run (X_{ALL}, where x=2000 or 2050 indicates the present

139   day or future, respectively) and a sensitivity run with no wildfire emissions to the atmosphere

140   (X_{WEF}, where X is the same as for the control runs). The ALL runs are designed to simulate

141   fully interactive fire disturbances such as fire emissions with plume rise and fire induced land

142   cover changes of the present day (representative of the 2000s, 2000$_{ALL}$) and a moderate future

143   emission scenario (representative of the 2050s, 2050$_{ALL}$) via the RCP4.5. The only difference

144   between the ALL and WEF scenario is that wildfire emissions are absent in the WEF

145   scenario. Specifically, in the WEF runs, the online simulated fire emissions are not passed to

146   the CAM5 atmosphere model so that the difference between the ALL and WEF runs can be

147   used to isolate the atmospheric impacts of fire-climate interactions.

148   Table 1: Summary of the sensitivity simulations performed

Scenario	Present-day		Future	
Experiment Name	2000$_{ALL}$	2000$_{WEF}$	2050$_{ALL}$	2050$_{WEF}$
Simulation years	2001-2010	2001-2010	2051-2060	2051-2060
Atmosphere	CAM5	CAM5	CAM5	CAM5
Land	CLM4.5	CLM4.5	CLM4.5	CLM4.5
Ocean	Climatology	Climatology	RCP4.5	RCP4.5
Sea ice	Climatology	Climatology	RCP4.5	RCP4.5
Non-fire emissions	ACCMIP	ACCMIP	RCP4.5	RCP4.5
Fire emissions	Online fire aerosols with plume rise	—	Online fire aerosols with plume rise	—
Land cover	Fire disturbances on present-day condition	Fire disturbances on present-day condition	Fire disturbances on RCP4.5 condition	Fire disturbances on RCP4.5 condition

149

150   For the present-day experiments, we used the spun-up states from Zou et al. (2019) as

151   initial conditions for both meteorological and chemical variables. Sea surface temperature

152   (SST) for the present day was obtained from the Met Office Hadley Centre (HadISST).

153   Present-day non-fire emissions from anthropogenic and other sources were based on

154   ACCMIP (Lamarque et al., 2010) for the year 2000. We replaced the prescribed GFED2 fire

155   emissions (van der Werf et al., 2006) in the default setting of CESM with the online-coupled

156   fire emissions generated by the RESFire model. Zou et al. (2019) provided more details of

157   the physics parameterizations and modeling experiment settings used in these simulations.

158 Land use and land cover data for 2000 and 2050 from the Land-Use History A product (Hurtt

159 et al., 2006) are used to initialize the 2000_{ALL}/2000_{WEF} and 2050_{ALL}/2050_{WEF} simulations,

160 respectively. Following the above setup, the future scenario 2050_{ALL} experiment accounts for

161 both fuel load changes associated with the projected land use and land cover change

162 (LULCC) in the 2050s and fire weather changes driven by the SST and sea ice forcing from a

163 coupled CESM simulation following the greenhouse gas (GHG) forcing of the RCP4.5

164 scenario. The global mean GHG mixing ratios in the CAM5 atmosphere model were fixed at

165 the year 2000 levels in all the present-day experiments and they were replaced by those of the

166 RCP4.5 scenario with the well-mixed assumption and monthly variations. However, the

167 future population and socioeconomic conditions were identical to those of the present day so

168 there was no explicit impact of human-induced mitigation/enhancement effects on wildfires

169 in the future projection in all the future experiments. Future human impacts were considered

170 implicitly in LULCC-induced fuel load changes in the RCP4.5 scenario.

171 The net projected changes by 2050s in emissions, meteorology and air quality during

172 summer (JJA: June, July, August) months are estimated by comparing decadal-mean values

173 simulated by 2000_{ALL} with 2050_{ALL}. Wildfire-induced enhancement in $PM_{2.5}$ concentration in

174 the present day and mid-21st century is estimated by comparing 2000_{ALL} with 2000_{WEF} and

175 2050_{ALL} with 2050_{WEF}, respectively. Further, the projected increase in wildfire-induced

176 $PM_{2.5}$ in the future is calculated by comparing the simulated wildfire effect of the 2050s

177 (2050_{ALL}-2050_{WEF}) with that of the 2000s (2000_{ALL}-2000_{WEF}). With large spatiotemporal

178 variability, the projected changes in transported fire-emissions from the western US and

179 Canada to the eastern US by the 2050s and the corresponding impacts are summarized using

180 probability distribution functions. The latter provide information not only for the mean but

181 also variability and extreme values to quantify the simulated changes for the three subregions.

182

3. Results and Discussion

3.1 Model Evaluation

Zou et al. (2019) performed comprehensive evaluation of the RESFire simulated wildfire burnt area distribution, associated carbon emissions and terrestrial carbon balance to demonstrate reasonable model skill. Zou et al. (2020) compares global fire simulations by CESM-RESFire with modeling results reported in the literature to show better agreement with the GFED4.1s benchmark data and predicts more prominent changes in the future than those predicted by Kloster et al. (2010, 2012). These differences might come from differences in the climate sensitivities of the fire models and scenarios and other input data used to make future projections.

Here, we evaluate the simulated surface $PM_{2.5}$ against satellite-estimates (Figure 1) over North America. The $PM_{2.5}$ concentration is calculated as the sum of sulfate, nitrate, fine sea salt (first 2 size bins), fine dust (first size bin), black carbon (BC), and organic aerosol (OC) at the surface-level of model. OC is the sum of primary organic matter (POM) and secondary organic aerosol (SOA), and SOA is the sum of secondary species formed from toluene, monoterpenes, isoprene, benzene, and xylene. Figure 1 compares the observed and simulated mean annual $PM_{2.5}$ averaged over 2001-2010. The 10-year average satellite AOD-derived annual mean surface $PM_{2.5}$ concentrations (Van Donkelaar et al., 2018) are regridded to the model grid (Figure 1A) and then compared with the RESFire simulations in the 2000_{ALL} present-day run (Figure 1B). The spatial distribution of annual surface $PM_{2.5}$ is reasonably well simulated but also have some biases. To quantify the biases, we also estimated the correlation coefficient as well as normalized mean biases (NMB) of the simulated values compared against the satellite retrieved values over two subregions. Quantitatively, the NMB values over the western US (WUS) and eastern US (EUS) are 18% and 7%, respectively (Figure 1C-D). In addition, the spatial variability of the 2001-2010

averaged annual AOD distribution (Supplementary Figure 1) is also well represented in our

simulation, although the model underestimates high AOD values. Similar spatial variability

and biases in AOD and $PM_{2.5}$ were also found when a comparison was performed for only

summer months (June through August; JJA). The simulated $PM_{2.5}$ has also been evaluated

against the ground-based Interagency Monitoring of Protected Visual Environments

(IMPROVE) data, showing similar spatial pattern and biases (10-25%) (Supplementary

Figure 2). The biases are smaller over Eastern US and Southwestern US region. The

simulated PM2.5 values over California matches quite well with the observed annual mean

values. However, the biases over Northwestern US region are ~30-40%, a portion of which

could be attributed to possible biases in model's meteorology in northwestern US region.

Nonetheless, both satellite and in situ evaluation indicate that our simulation biases are

largely within the uncertainty range among the various satellite and ground-based datasets,

which have normalized mean biases ranging from -3.3% to 33.3% when benchmarked against

the ground-based IMPROVE data over the contiguous US (Diao et al., 2019; Val Martin et al.

(2015)).

Discrepancies between the simulated and observed $PM_{2.5}$ values may be attributed to

several potential reasons. First, the satellite-derived data has a non-zero lower bound of $PM_{2.5}$

concentrations, so the ambient background concentrations for relatively cleaner regions such

as the western US may be overestimated (Figure 1C), also the sampling frequency between

these datasets are different. Second, year 2000-based constant non-fire emissions were used

in the RESFire simulation, which may result in overestimation of the $PM_{2.5}$ concentrations

from non-fire sources during 2001-2010 when anthropogenic emissions and $PM_{2.5}$

concentrations continue to decrease (US EPA, 2018). This overestimation is prominent in

regions dominated by non-fire sources such as the southeastern US. Third, large uncertainties

in fuel consumption and emission factors preclude an accurate estimation of the primary fire

233   emissions in the model, especially for the eastern US where large fractions of low-intensity

234   prescribed fires consume only under-canopy fuels such as litter and duff layers. The fire

235   model may fail to capture the subtle distinctions between low-intensity prescribed fires and

236   forest fires, so more fuels are consumed and result in higher emissions. Lastly, comparison of

237   a coarsely resolved simulation against in-situ observations also contributes to uncertainty.

238   Differences in the degree to which fire-climate interactions and other physical processes and

239   feedbacks are represented by the models can explain the slights differences in estimating the

240   present day mean wildfire-induced change in $PM_{2.5}$ over local and downwind regions

241   between our simulations and previous studies. Nonetheless, reasonable simulation of the

242   spatial distribution of wildfire burnt area, AOD, and near surface particulate concentration

243   (mean bias of ~10-20 %) instills confidence about the fidelity of our model setup in

244   particulate pollution simulation, which is the focus of this study.
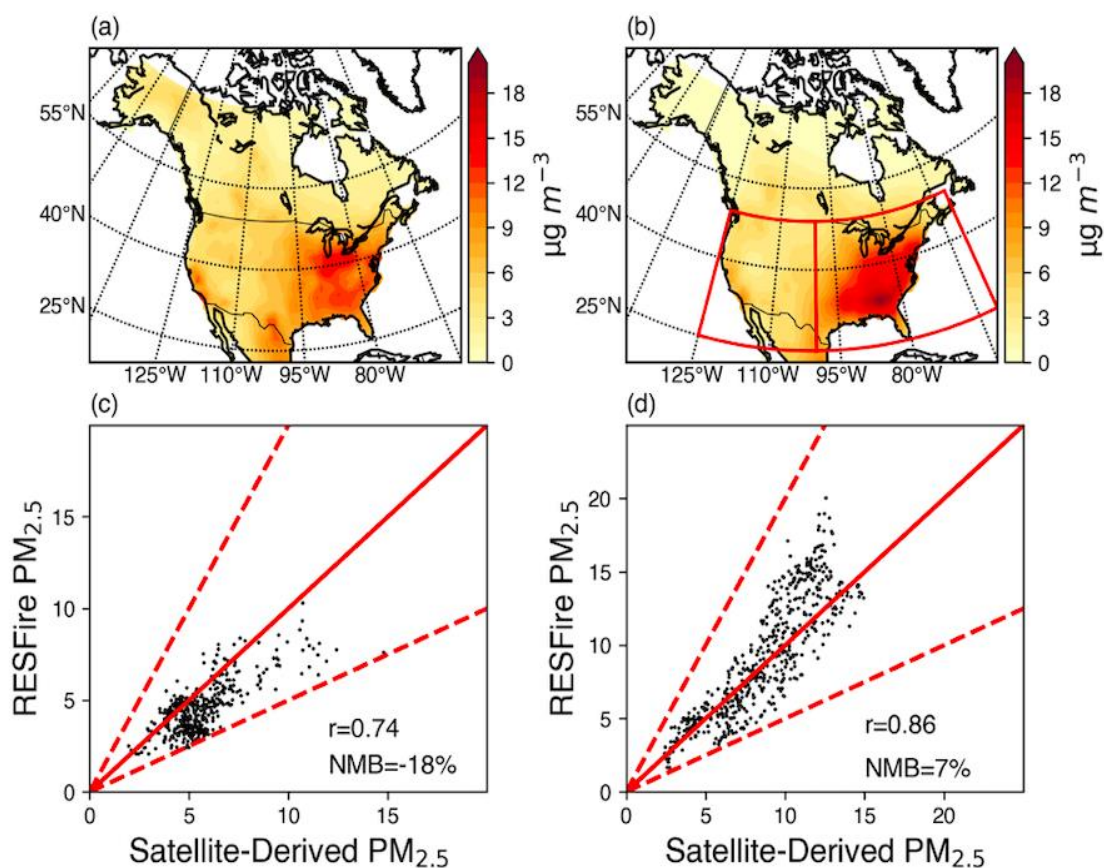
245

246

247 Figure 1: Comparison of the 10-year (2001-2010) averaged annual mean surface $PM_{2.5}$
248 concentration between observations and RESFire simulations. (a) Satellite-derived surface
249 $PM_{2.5}$ concentrations (with dust and sea-salt removed) estimated by Donkelaar et al., 2018
250 (available at https://sedac.ciesin.columbia.edu/data/set/sdei-global-annual-gwr-pm2-5-modis-
251 misr-seawifs-aod; last access: 5 November, 2021); (b) 2000$_{ALL}$ Simulated surface $PM_{2.5}$
252 concentrations (with dust and sea-salt removed) averaged over 2001-2010; The red boxes
253 denote the two subregions (EUS and WUS) shown in Fig. 2 in the main text. (c) comparison
254 of simulated and satellite based gridded surface $PM_{2.5}$ concentrations in the WUS subregion;
255 Number of samples is equal to the number of land grids ~450 (d) same as (c) but in the EUS
256 subregion. Number of samples is equal to the number of land grids ~375 The red solid and
257 dashed lines denote the 1:1 ratio line and $\pm100\%$ biases, respectively. The correlation
258 coefficients and NMB values are shown at the lower-right corner of each subplot.

259

260 **3.2 Fire-induced changes in burnt area and $PM_{2.5}$**

261   The decadal-mean annual fire burnt area simulated for the present day shows

262 widespread wildfires over the entire North America (Figure 2A). Specifically, Canada and the

263 forested areas of the northwestern (> 36 N latitude) and southeastern (< 36 N latitude) US are

264 most intensely affected by wildfires in the present day. By the mid-21st century, a striking

265 increase of 2-5 times in fire burnt area is projected over Canada, Alaska, the Pacific

266 Northwest and portions of the western US by the 2050s (Figure 2B). A distinct positive shift

267 in the probability density function (PDF) of annual fire burnt area is evident in the future,

268 with the decadal-mean difference statistically significant at the 99% confidence level (Zou et

269 al., 2020). A small and statistically insignificant change in interannual variability (~ 0.4 Mha

270 yr^{-1}) of fire burnt areas is also simulated between the present and future. Specifically, our

271 model predicts more than a doubling of burnt area in boreal regions of Canada in the future,

272 in line with a previous projection for Canada (Wotton et al., 2017). Future enhancement in

273 fire burnt area is ~ 20-50% in most fire grids over the western coast of US, which is higher

274 than that over the eastern US (Figures 2A and 2C). The increase over the western US is closer

275 to the lower bound of that derived from statistical model ensemble projections for the western

276 US in the mid-21st century (Yue et al., 2013). The statistics-based projections of future burnt

277   area over North America were likely too high because fire-induced land cover change, fuel

278   load reduction and factors could induce a negative fire feedback, which was not considered in

279   previous fire projection studies (Zou et al. 2020).

280   Annual fire burnt area in the southeastern US shows a decline in the future (Figure

281   2C), as precipitation is projected to increase in that region (discussed later). Note that all

282   future fire changes between 2050_{ALL} and 2000_{ALL} are primarily associated with climate

283   warming in response to the increase in greenhouse gas (GHG) concentrations in the RCP4.5

284   scenario. No direct impacts of population and socioeconomic changes on wildfires are

285   included in our simulations, although these factors contribute to changes in GHG emissions

286   (via the RCP scenario) that influence the climate simulated in 2000_{ALL} and 2050_{ALL}. As about

287   80% of the projected fire changes in the future is restricted to the summer season (June

288   through August; JJA) (Figure 2D), we focus on analysis of the summer-mean wildfire-

289   induced $PM_{2.5}$ and its projected future changes over North America.

290
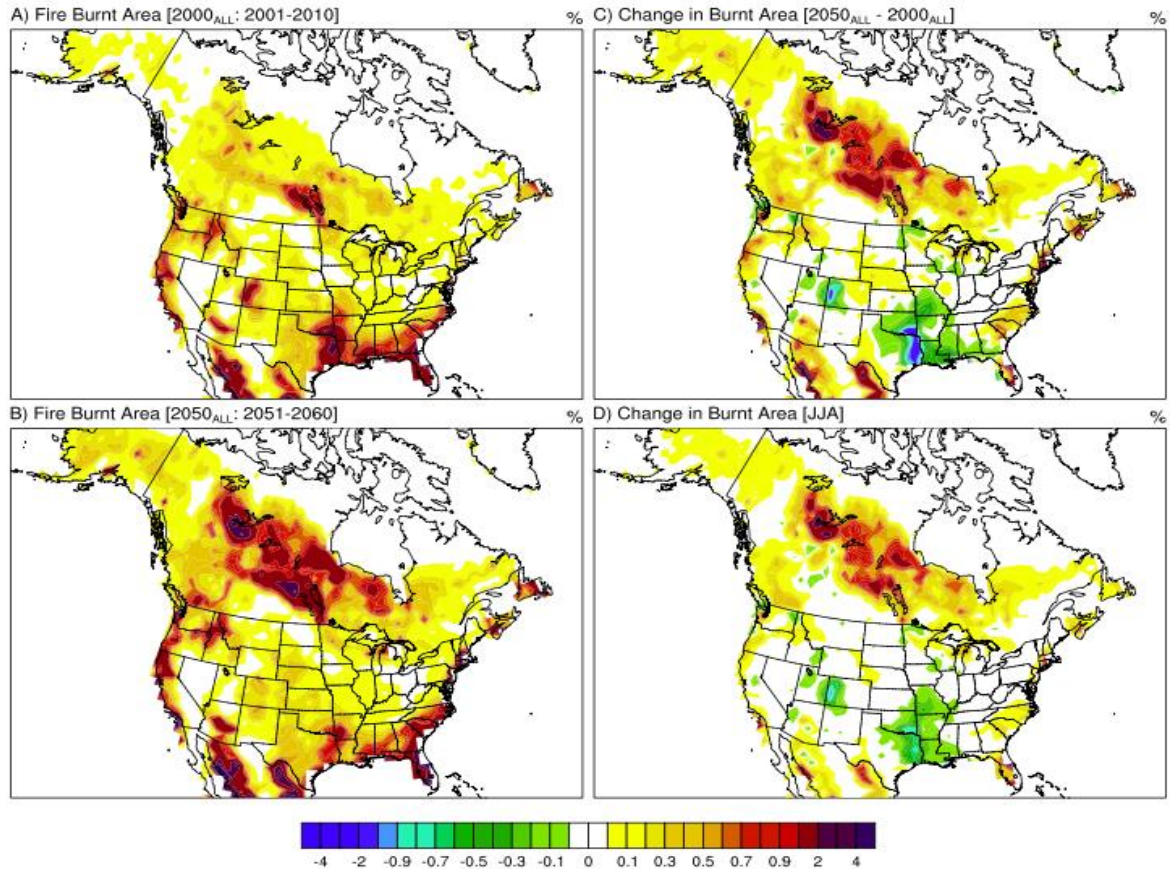
Figure 2: **Spatial distribution of fire burnt area. A-D**, Spatial distribution of simulated decadal-mean annual burnt area (as percentage) over North America for present day (A), mid-21st century (B) and the net change between the 2050s and the 2000s (C). **D**, same as (C), but for wildfire burnt area during summer only (June through August; JJA). The colorbar illustrate grid fraction of area burnt.

The simulated 10-year averaged summer-mean wildfire-induced $PM_{2.5}$ values in

2000_{ALL} are more than 0.5 µg/m^3 over a large part of North America in the present day, with

noticeably larger values (> 1 µg/m^3) in Canada and the northwestern, central, and

southeastern US (Figure 3A). Interestingly, the spatial distribution of wildfire-induced

$PM_{2.5}$ > 1 µg/m^3 resembles an inverted horse-shoe shape. The inverted horse-shoe shaped

spatial distribution is also consistent with the wildfire-smoke climatology derived from the

satellite-guided operational smoke product of the Hazard Mapping System (HMS) during

2005-2015 (Brey et al., 2018; Kaulfus et al., 2017). By the mid-21st century, the spatial extent

of the horse-shoe shape for areas with wildfire-induced $PM_{2.5}$ enhancement > 1 µg/m^3

306   expands significantly to span most regions of North America, with the most pronounced

307   enhancement occurring over Canada (Figure 3B). The PDFs of the spatial distribution for the

308   three regions can be seen in Figure 3C-E. Specifically, wildfire induced $PM_{2.5}$ in the 2000s

309   over Canada, WUS and EUS during summer is ~ 1-3 µg/m^3, 1-3 µg/m^3 and 0.6-1.2 µg/m^3,

310   respectively. Maximum values within the WUS region are found over the Pacific Northwest,

311   with most areas having wildfire induced $PM_{2.5}$ values of ~ 2-3 µg/m^3. Similarly, the southern

312   states have relatively high wildfire induced $PM_{2.5}$ concentrations of ~ 2-4 µg/m^3 within the

313   EUS in the present-day simulation.

314   Compared to the 2000s, the wildfire induced JJA-averaged $PM_{2.5}$ values are almost

315   doubled to ~ 3-6 µg/m^3 over Canada in the 2050s (Figure 3B and Figure 3C). Consistently,

316   the values of wildfire induced PM2.5 over WUS (mainly coastal) also doubled in 2050s

317   compared to 2000s, with modal values of ~ 2-2.5 µg/m^3 (Figure 3D). Most interestingly, the

318   enhancement in wildfire-induced summer-mean $PM_{2.5}$ over the northern EUS is also

319   significant by the 2050s (Figures 3B). Largely, the summer-mean wildfire-induced $PM_{2.5}$

320   concentration over EUS increases from ~0.8 to ~2 µg/m^3 in the mid-century to values of 1.2-

321   3.0 µg/m^3 (Figure 3E). The summer-mean wildfire-induced $PM_{2.5}$ is thus projected to double

322   in North America by the 2050s compared to the 2000s, with a substantial coverage over the

323   EUS. An important finding from these PDFs appears to be that there are fewer grids with < 1

324   µg/m^3 wildfire induced PM2.5, or alternatively, that more regions are being influenced by

325   PM$_{2.5}$, and many areas that were already seeing wildfire impacts are seeing enhanced

326   impacts. Such enhancement is found not only at the surface but also in an elevated

327   atmospheric layer over EUS between 900 and 700 hPa. This is nonintuitive given the fact that

328   the increase in fire-burnt area by mid-century over the EUS is not substantial.
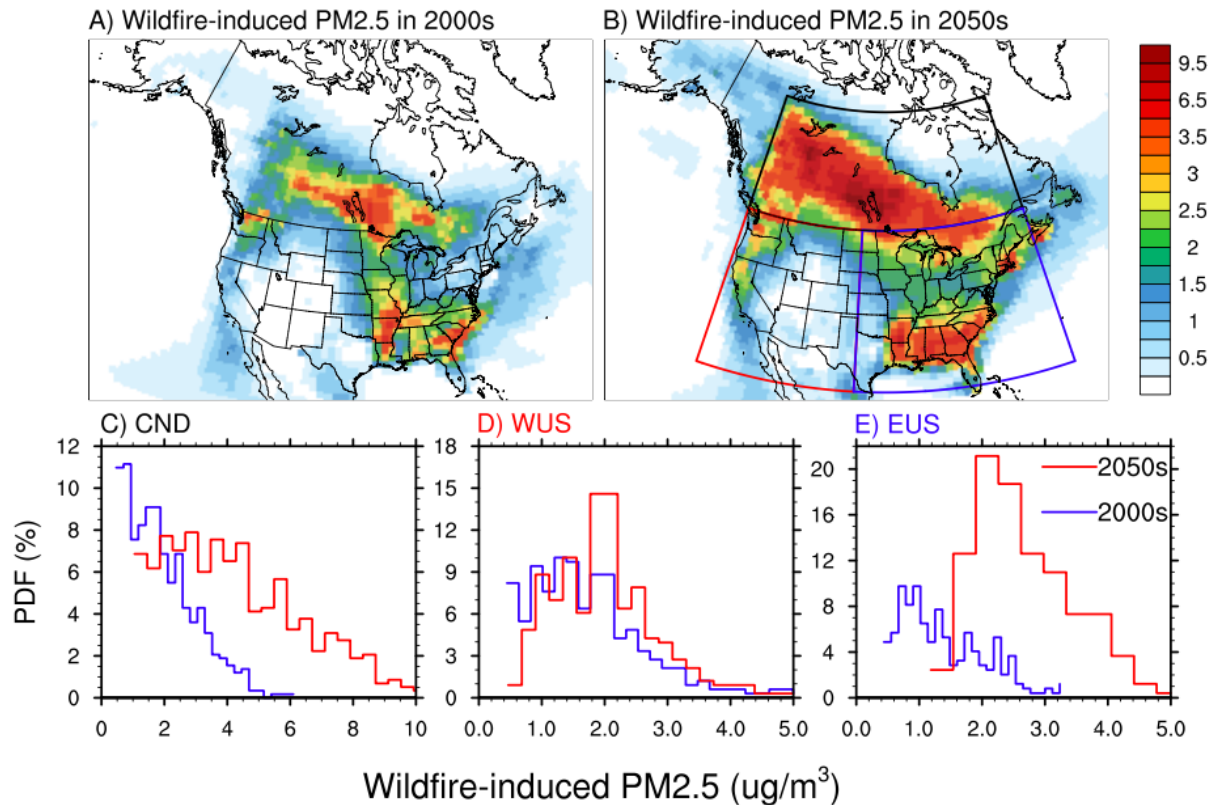
Figure 3: **Spatial distribution of** PM2.5 **concentrations.** Spatial distribution of decadal-mean wildfire-induced enhancement in summer (June through August; JJA) PM2.5 concentration over North America for present day (A, 2000ALL-2000WEF) and future (B, 2050ALL-2050WEF). **C-E**, Probability density functions (PDFs) of wildfire contribution within the three regions shown in Figure 2B for Canada (CND: black box) (C), WUS (red box) (D), and EUS (blue box) (E), respectively, for 2000s (blue) and 2050s (red). Only grids over land in North America are used to generate the PDFs. The y-axis indicates the probability of occurrence of different PM2.5 values shown in the x-axis. The colorbar illustrates PM2.5 in ug/m^3.

As anthropogenic- and wildfire-induced PM2.5 concentrations may change differently with time across North America, next, we investigate the relative contribution of wildfire-induced PM2.5 to the total PM2.5 in the future. Prominent enhancement of the wildfire contribution is apparent in the entire domain by the 2050s (Figures 4A-B). Largely, during the 2000s, the simulated fractional contribution of wildfires to PM2.5 is ~15-50 % in Canada (Figure 4A). Specifically, a bi-modal distribution is simulated over Canada with modal values around 18% and 30% (Figure 4C). Over WUS, the present day simulated percentage contributions of wildfire-induced values are 5-25% (Figure 4A), with modal values between

347 10-20% (Figure 4D). Note that many areas located in the Pacific Northwest have higher

348 values of ~30-40% (Figure 4A). At the same time, the fractional contribution by wildfire-

349 induced PM$_{2.5}$ is ~5-10% in most areas of EUS in present day (Figure 4F). Nevertheless,

350 some areas in the central US also have higher values of ~10-25% (Figure 4A).
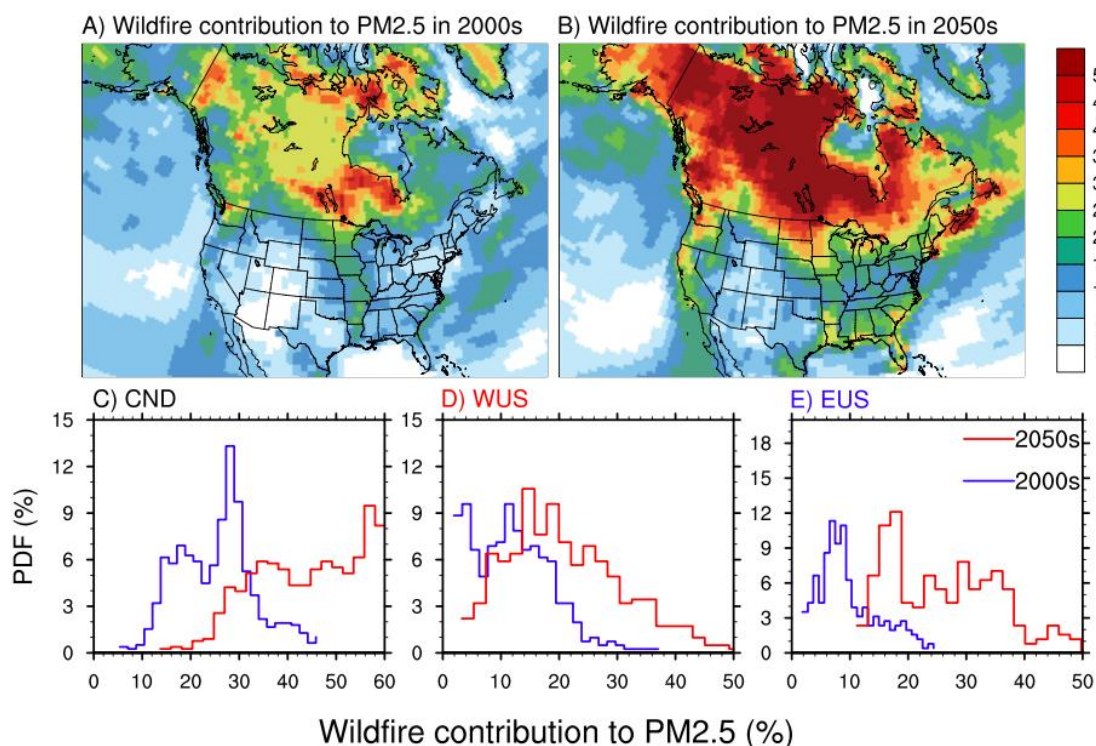
352 Figure 4: **Spatial distribution and probability density function of the percentage**
353 **contribution of wildfire emissions. A-B**, Spatial distribution of the percentage contribution
354 of wildfire emissions to decadal-averaged summer (June through August; JJA) mean PM$_{2.5}$
355 concentrations over North America during present day (A) and future (B). The percentage
356 contribution of wildfire-induced PM$_{2.5}$ to the total PM$_{2.5}$ concentrations is calculated as
357 ([2000$_{ALL}$-2000$_{WEF}$]/2000$_{ALL}$) and ([2050$_{ALL}$-2050$_{WEF}$]/2050$_{ALL}$) for the present and future,
358 respectively. **C-E**, Probability density functions (PDFs) of the percentage wildfire
359 contribution within the three regions shown in Figure 2D for Canada (CND: black box) (C),
360 WUS (red box) (D), and EUS (blue box) (E), respectively, for the 2000s (blue) and the 2050s
361 (red). Only grids over land in North America are used to generate the PDFs. The y-axis
362 indicates the probability of occurrence of different PM$_{2.5}$ values shown in the x-axis.

364   The wildfire contributions in the 2050s show a clear shift towards higher values in all

365 sub-regions compared to the 2000s (Figure 4B). Over Canada, the values shifted from 15-30

366 % in the 2000s to ~30-60% in the 2050s, a nearly two-fold increase in the fractional

367 contribution of wildfire emissions to the total $PM_{2.5}$ concentration is simulated (Figure 4B

368 and corresponding PDF in Figure 4C). Similarly, the contribution values increased to ~ 10-35

369 % in the 2050s, compared to 10-20% in the 2000s over WUS (Figure 4B), thereby featuring a

370 broadening of the bi-modal distribution of wildfire contribution (Figure 4D). The shift in the

371 percentage contribution is most prominent for the higher values, corresponding to some areas

372 located in the Pacific Northwest and west coast of the US (Figure 4B). Consistent with Figure

373 3B, the shift in the contribution values over EUS is also very distinct, revealing an increase in

374 the mode values from 6-10% in the 2000s to ~16-20 % by the 2050s (Figure 4B and Figure

375 4E). Thus, not only in absolute values, but our results also underscore a large increase in the

376 contribution of wildfire emissions over EUS in the future.

377 **3.3. Mechanistic understanding of the underlying processes**

378 The larger enhancement in the relative contribution of wildfire emissions to the total

379 surface $PM_{2.5}$ in EUS in the 2050s can be explained by three mechanisms. First, due to the

380 increase in Canadian and western US wildfires, downwind transport of wildfire smoke

381 plumes to EUS will be enhanced by the 2050s. This long-range transport to the atmospheric

382 column of EUS can happen within a few days of the fire occurrence (Supplementary Figures

383 3A and 3B). Using Hazard Mapping System (HMS)-detected smoke plumes, recent studies

384 identified a strong positive association between the transported smoke plumes in the

385 atmospheric column and collocated surface PM2.5 enhancement in EUS (Brey et al., 2018;

386 Wu et al., 2018; Gunsch et al., 2018; Kaulfus et al., 2017; Larsen et al., 2017; Dempsey,

387 2013). Hazard Mapping System (HMS) is an operational smoke detection product over North
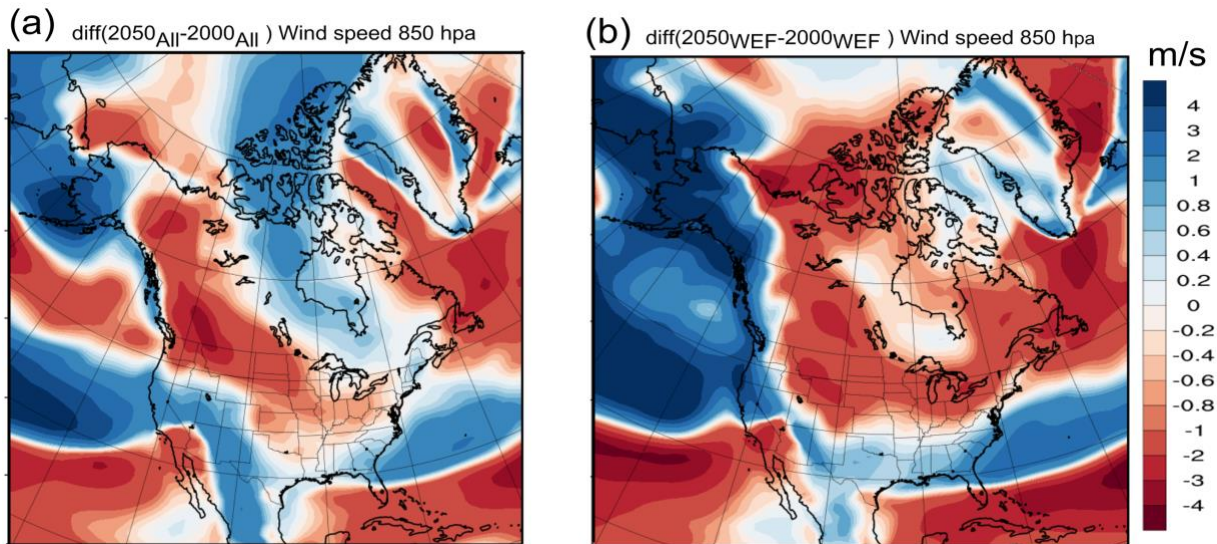
Figure 5a: Spatial distribution of decadal mean summer (June through August; JJA) wildfire-induced future changes [(2050$_{ALL}$-2050$_{WEF}$) – (2000$_{ALL}$-2000$_{WEF}$)]. A) Wind speed at 850 hpa for [(2050$_{ALL}$- – 2000$_{ALL}$], B) Wind speed at 850 hpa [(2050$_{WEF}$) – (2000$_{WEF}$)].

America known as developed by the National Oceanic and Atmospheric Administration

(NOAA) and operated by National Environmental Satellite, Data, and Information Service

(NESDIS), available at http://satepsanone.nesdis.noaa.gov/FIRE/fire.html. Specifically, these

studies found that the smoke plumes transported from Canada are located at an altitude of ~

1-3 km over EUS (Colarco et al., 2004; Wu et al., 2018). Due to mixing by the daytime

boundary layer and deposition, the smoke plumes enhance the surface PM$_{2.5}$ concentration

over EUS (Wu et al., 2018; Colarco et al., 2004; Rogers et al., 2020; Dreessen et al., 2015).

Hence HMS smoky days may be a useful proxy for wildfire-induced surface PM2.5 over

North America. In agreement, Brey et al. (2018) showed that the HMS-based smoke plumes

observed over EUS is significantly aged, suggestive of their long-range transport origin.

Consistent with the observed temporal change in HMS pattern, Xue et al. (2021) estimated

using the mid-visible Multi Angle Implementation of Atmospheric Correction (MAIAC)

satellite-derived Aerosol Optical Depth (AOD) that Canadian and western US fires have

caused an increase in the daily PM$_{2.5}$ over Montana, North Dakota, South Dakota and

Minnesota by 18.3, 12.8, 10.4 and 10.1 $\mu g\ m^{-3}$, respectively, between August 2011 (a low

407   fire month) and August 2018 (a high fire month). In summary, the visually apparent satellite-

408   based signatures of wildfire-smoke across Canada and EUS provide a necessary, though not

409   sufficient, support for the influence of Canadian smoke plumes on EUS air quality. Although,

410   the change in burnt area over northeastern EUS is negligible compared to the western US and

411   Canadian regions, however, there are some enhancements seen over east coast of US, which

412   can also contribute to enhanced fire emissions.

413   In future, the simulated speed of the westerly jet flows over Canada wildfire regions is

414   reduced in both the scenarios (Figure 5 A-B). It indicates that the westerly-induced

415   transported wildfire emissions from Canada boreal forests to the eastern half of Northern

416   America and EUS will be slower in future compared to that in present era. On the one hand, it

417   implies that the advection of smoke plumes will be slightly reduced in future. But on the

418   other hand, this phenomenon can also contribute to the enhanced PM2.5 values at surface as

419   these transporting plumes will be subject to relatively more boundary layer mixing over the

420   EUS and dry deposition/settling enhances. At the same time, the westerly winds over western

421   US below 40 ^{o}N is strengthened in future (Figure 5 A-B) compared to present day which

422   indicates more advection flux of wildfire emissions to EUS. Thus, the net effect is more

423   removal of wildfire-emitted PM2.5 from WUS and more influx of wildfire-emitted PM2.5 in

424   EUS.

425   Along with this dynamical changes, other climatic feedbacks simulated can also contribute to

426   enhancement of EUS pollution. Specifically, the enhancement of wildfire-induced smoke

427   aerosols increases solar absorption and scattering in the future (Figure 6A). This reduces the

428   incoming solar radiation reaching at the surface (Figure 6B) and induces surface cooling.

429   With atmospheric warming and surface cooling, lower-tropospheric stability is enhanced by

430   wildfire aerosols in the future (Figure 6C). The smoke plumes which reaches eastern US are

431   at an elevated altitude due to self-lofting property of absorbing aerosols as they travel

432   downwind but the smoke over western US is at near surface elevation as it is at its source

433   region. This can explain the more significant atmospheric stability simulated over the eastern

434   US compared to the source regions in western US and boreal forests of Canada. Relatively

435   stronger atmospheric stability over eastern US impose a stronger thermal capping that traps

436   more anthropogenic aerosols and particulate matter near the surface over EUS (already an

437   emission hotspot). At the same time, future increase in wildfire emissions also leads to

438   greater reduction of monthly rainfall (Figure 6D) over EUS, which may additionally

439   strengthen the positive feedback to surface $PM_{2.5}$ over EUS by reducing wet scavenging of

440   transported wildfire smoke to EUS. Thus, wildfire-emitted aerosols induce positive feedback

441   on the surface $PM_{2.5}$ concentration over EUS through fire-climate interactions that vary on a

442   regional scale. Moreover, the above discussed dynamical changes in future can also feedback

443   these simulated thermodynamical and precipitation changes, exaggerating the enhancement in

444   PM2.5 values over EUS in future. However, due to computational constrains, no direct

445   quantification of the magnitude of these feedback (with aerosol-radiation and aerosol-cloud

446   interactions turned off) on PM2.5 is performed and would be taken up in future studies.

447   Lastly, the reason of why the contribution of wildfire emissions to the total surface

448    $PM_{2.5}$ in EUS is so substantial in the 2050s is the drastic reduction of anthropogenic

449   contribution to the surface $PM_{2.5}$ over EUS in the future primarily due to policy-driven

450   reduction in anthropogenic emissions under the RCP4.5 scenario. Specifically, the simulated

451   ambient summer mean $PM_{2.5}$ concentration exhibits widespread declines in the future

452   (Supplementary Figure 4), with reduction in $PM_{2.5}$ concentration over eastern US in the range

453   of 4-15 $\mu g/m^3$, which is greatest within North America. Thus, large reduction in

454   anthropogenic contribution combined with increased downwind advection of Canadian

455 smoke to EUS and the associated positive feedbacks can explain the projected dominance of

456 wildfire emissions over EUS in future.
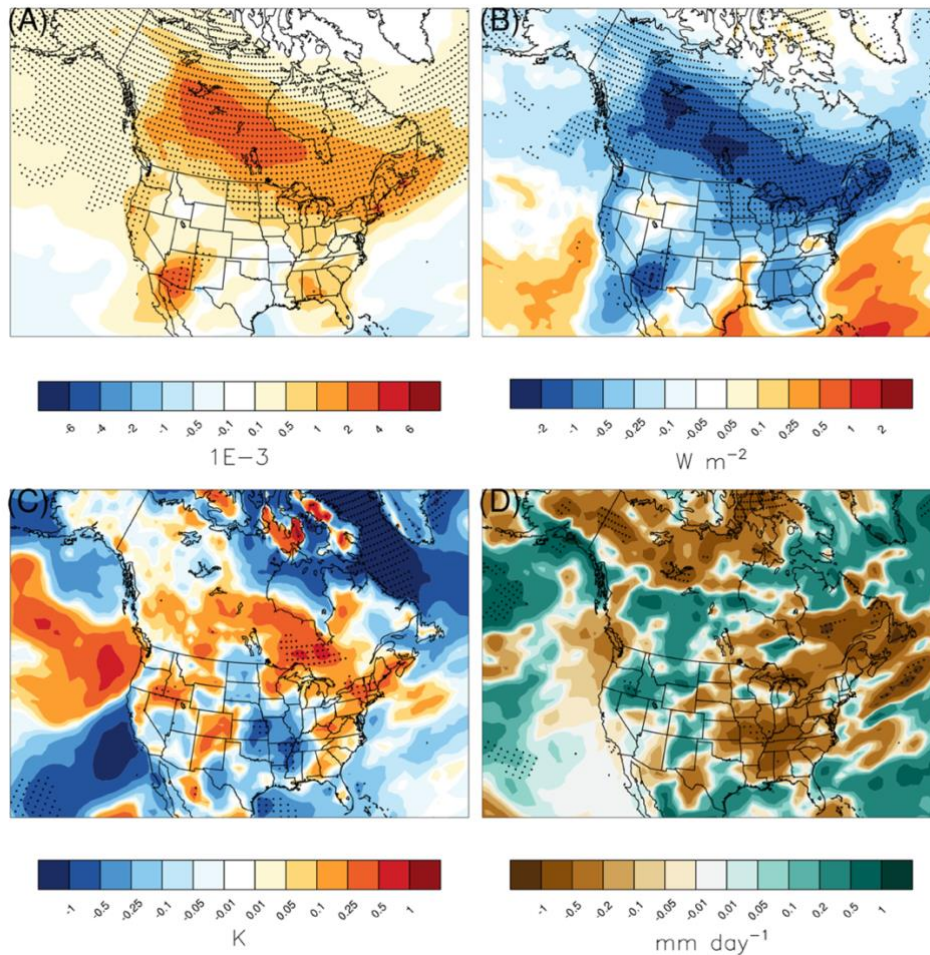
457

458 Figure 6: Spatial distribution of decadal mean summer (June through August; JJA) wildfire-
459 induced future changes [(2050$_{ALL}$-2050$_{WEF}$) – (2000$_{ALL}$-2000$_{WEF}$)]. A) aerosol absorption
460 optical depth at 550 nm, B) aerosol direct radiative forcing at surface, C) lower-tropospheric
461 stability calculated as the difference between the potential temperature at 900 hPa and 1000
462 hPa, D) summer averaged precipitation rates, over North America. Areas marked with black
463 dots indicate grids where changes are significant at the 95% confidence level.

464

3.4 Future Implications and uncertainties

466   However, is the simulated future enhancement in wildfire contribution over EUS

467 substantial enough to affect the surface PM$_{2.5}$ values over EUS in future? The World Health

468 Organization (WHO) air quality guidelines for annual and daily PM$_{2.5}$ concentration are 10

469 $\mu g\ m^{-3}$ and 25 $\mu g\ m^{-3}$, respectively. As no specific guideline for seasonal-mean PM$_{2.5}$ in the

470   summer is available, we use the annual guideline value as a reference to understand the

471   implication of wildfire emissions on ambient $PM_{2.5}$ concentration in the future. Interestingly,

472   the mean summertime $PM_{2.5}$ concentration in the wildfire emission free (WEF) scenario is

473   projected to remain within 10 µg m^{-3} over most of North America, except for the

474   southeastern US (~15% of the domain) (Figure 7A). However, the ALL-scenario projects an

475   increase in the exposure concentration level such that values > 10 µg/m^3 are common in

476   Canada and EUS in the future (Figure 7B). Quantitatively, over Canada, the entire PDF of

477      $PM_{2.5}$ concentration shifts towards higher values by ~5-6 µg/m^3. Specifically, the modal value

478   shifts from ~ 6 µg/m^3 in 2050$_{WEF}$ to 11-12 µg/m^3 in 2050$_{ALL}$ (Figure 7C), so $PM_{2.5}$

479   concentration is projected to surpass the WHO guidelines over a large fraction of Canada in

480   the future. Similarly, the entire PDF of $PM_{2.5}$ concentration shifts towards higher values by

481   ~2-3 µg/m^3 over EUS, with the mode of the PDF increasing from ~ 7-8 µg/m^3 in 2050$_{WEF}$ to

482   ~ 10-11 µg/m^3 in 2050$_{ALL}$ (Figure 7E). The modal value of summer mean $PM_{2.5}$ over WUS

483   increases from ~ 6 µg/m^3 in 2050$_{WEF}$ to ~ 7-8 µg/m^3 in 2050$_{ALL}$ (Figure 7D), although a few

484   grid cells show $PM_{2.5}$ values greater than 10 µg/m^3 (Figure 7B).

485   Clearly, the climate-induced enhancement in fires and its influence via the advected

486   wildfire smoke to EUS can have significant implications for air quality management in the

487   future. The PM2.5 enhancement in future over the southern states within EUS is large (Figure

488   7A-B), which is consistent with Figure 3 and 4 results. However, the future change in burnt

489   area over the same region is negligible or mostly reducing (Figure 1C-D). Thus, it can be

490   argued that the simulated enhancement is mostly related with the dynamic perturbations and

491   thermodynamical feedbacks due to wildfire emissions (Figure 6). As the rate of

492   anthropogenic emissions is also regionally highest over the Southeastern states, the impact of

493   these wildfire-induced climatic feedbacks on local air quality is distinctly seen over the EUS.

494
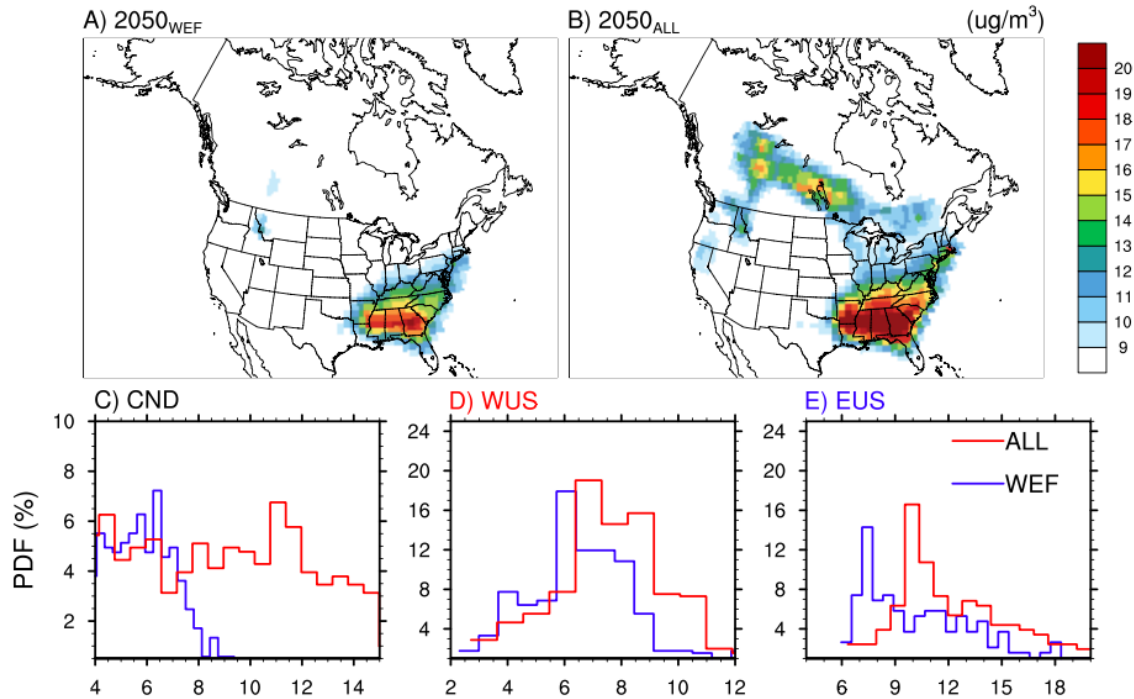
Figure 7: **Spatial distribution and probability density function of** PM$_{2.5}$ **concentration in**
2050s. A-B, Spatial distribution of decadal-average summer (June through August; JJA)
mean PM$_{2.5}$ concentration over North America in mid-21st century from 2050$_{WEF}$ (wildfire
emission-free) (A) and 2050$_{ALL}$ (wildfire emission-inclusive) (B). **C-E**, Probability density
functions (PDFs) of the same within the three regions shown in Figure 2B for Canada; CND
(C), western US; WUS (D), and eastern US; EUS (E), respectively, for the 2050$_{WEF}$ (blue)
and 2050$_{ALL}$ (red) runs. The y-axis indicates the probability of occurrence of different PM$_{2.5}$
values shown in the x-axis. Only grids over land in North America are used to generate the
PDFs. Note the different ranges of values shown in the y- and x-axis in **C-E**. The colorbar
and the x-axis for Panel C-E indicates PM$_{2.5}$ values.

Note that our simulated present-day estimates of wildfire induced PM$_{2.5}$ values as well

as the percentage contribution of wildfire emissions are within the range of reported values in

previous studies over the domain, which augment the fidelity our future projections.

Specifically, our simulated present-day estimates of wildfire induced PM$_{2.5}$ values are also

within the range of reported values in previous studies over the domain. Reported values of

wildfire-induced PM$_{2.5}$ over WUS during summertime vary from ~1 µg/m^3 (Jaffe et al., 2008)

to ~2 µg/m^3 (Park et al., 2007) and ~3 µg/m^3 (Ford et al., 2018), with the highest values

documented over the Pacific Northwest and west coast regions (~1-4 µg/m^3) (O'Dell et al.,

2019). The wildfire-induced PM$_{2.5}$ over EUS during summertime varies from ~1 µg/m^3 (Park

514   et al., 2007) to ~2.5 µg/m^3 (~ 3 µg/m^3 in the southeastern US) (Ford et al., 2018).

515   Consistently, our simulated present-day estimates of wildfire contribution values are also

516   within the range of reported values in previous studies. For example, Meng et al. (2019)

517   found that wildfires can be the largest sectoral contributor (~18-59%) to the population-

518   weighted PM$_{2.5}$ in various subregions of Canada. Over WUS, the present-day percentage

519   contribution of wildfire induced PM$_{2.5}$ to the total PM$_{2.5}$ is reported to be ~ 12% (Liu et al.,

520   2017), ~ 15% (Park et al., 2007) and ~30% (Ford et al., 2018), with higher values of ~40% in

521   the Pacific Northwest (O'Dell et al., 2019). Over EUS our simulated values are also within

522   the range of previously reported values of ~ 5% (Park et al., 2007) and ~15-18% (Ford et al.,

523   2018). However, our two-way coupled simulations illustrate that future enhancement in the

524   wildfire associated PM$_{2.5}$ over the EUS could be greater compared to the western US, which

525   is not emphasized explicitly in any of the previous studies (although Ford et al., 2018

526   illustrated increase in PM2.5 over mid and central US from Canadian fires). These could be

527   since inclusion of the wildfire-induced climatic feedbacks in our simulation is an

528   unprecedented exercise. Please also note that our study is focused on JJA period and the

529   wildfires in western US mainly occurs during August-September months, so the results

530   should be compared consciously.

531   Nonetheless, inherent limitations in our simulations may introduce uncertainties in the

532   projected future changes. For example, our reported changes in PM$_{2.5}$ concentrations based on

533   relatively coarse resolution simulations and decadal averages likely represent a low-end

534   estimate compared to changes at regional and daily/weekly scales. Moreover, our

535   experiments do not consider the direct human influences such as population change and

536   socioeconomic development on wildfires, which may aggravate the increase in PM$_{2.5}$

537   concentrations over the densely populated EUS in the future. Common sources of uncertainty

538   in modeling burnt area and fire emission and fire aerosol and smoke are also present in our

539   model. Fire smoke, in particular, is extremely hard to measure and evaluate. Lastly, inherent

540   uncertainties in the physics parameterizations used in the model, sensitivity of climate to

541   GHGs emissions, and the RCP scenarios should also be noted. Thus, ensemble modeling

542   considering different emissions scenarios, population and future time periods, and the use of

543   a finer spatial resolution may provide a more robust and better quantification of the wildfire-

544   induced impact on policy regulated improvements in $PM_{2.5}$ over EUS.

545   **4. Conclusion**

546   In summary, online coupled fire-climate-ecosystem simulations project a nearly

547   twofold increase in wildfire-induced summer-mean surface $PM_{2.5}$ concentration by the mid-

548   21st century over the entire North America. In a wildfire-emission free future, a large portion

549   of North America will have $PM_{2.5}$ values below the WHO guidelines. But in a future with

550   wildfire emissions, the improvements from policy-driven reductions in anthropogenic $PM_{2.5}$

551   will be compromised by the projected doubling of $PM_{2.5}$ from wildfires. More strikingly,

552   wildfire-induced enhancement in surface $PM_{2.5}$ values and percentage contribution of the

553   wildfire emissions over EUS could be substantial by mid-century. This is mainly because of

554   the large enhancement in fires over Northern America by 2050s and associated increase in

555   amount of downwind transport of smoke to EUS. In addition, enhancement of smoke

556   transport induces a positive climate feedback to $PM_{2.5}$ concentrations over EUS by increasing

557   the lower-tropospheric stability and reducing wet scavenging rates. Despite the inherent

558   limitations, this study highlights the natural versus anthropogenic contributions and the non-

559   local nature of air pollution that can complicate regulatory strategies aimed at improving air

560   quality over the eastern US in a warmer future.

561   **Data availability statements**

The HMS data used in this paper are available free through the link
https://www.ospo.noaa.gov/Products/land/hms.html. The model simulations data are
available at https://portal.nersc.gov/project/m1660/yang560/wildfire

Code availability statements

The model code and scripts are available at
https://portal.nersc.gov/project/m1660/yang560/wildfire

Acknowledgements:

This research was performed at PNNL and funded under Assistance Agreement No.
RD835871 by the U.S. Environmental Protection Agency to Yale University through the
SEARCH (Solutions for Energy, AiR, Climate, and Health) Center. It has not been formally
reviewed by EPA. The views expressed in this document are solely those of the SEARCH
Center and do not necessarily reflect those of the Agency. EPA does not endorse any
products or commercial services mentioned in this publication. CS is supported by the New
Faculty Initiation Grant project number CE/20-21/065/NFIG/008961 from IIT Madras.
PNNL is operated by Battelle Memorial Institute for the U.S. Department of Energy under
contract DE-AC06-76RLO-1830.

Authors Contribution

YQ, CS and RL designed this study. CS did the model and satellite analysis and wrote the
first draft of the manuscript. YZou performed the simulations. All authors provided inputs
throughout the study and helped in the drafting and submission process.

References

Abatzoglou, J. T. and Williams, A. P.: Impact of anthropogenic climate change on wildfire
across western US forests, Proc. Natl. Acad. Sci., 113(42), 11770 LP – 11775,
doi:10.1073/pnas.1607171113, 2016.

Andela, N., Morton, D. C., Giglio, L., Chen, Y., van der Werf, G. R., Kasibhatla, P. S.,
DeFries, R. S., Collatz, G. J., Hantson, S., Kloster, S., Bachelet, D., Forrest, M., Lasslop, G.,
Li, F., Mangeon, S., Melton, J. R., Yue, C. and Randerson, J. T.: A human-driven decline in
global burned area, Science (80-.)., 356(6345), 1356 LP – 1362,
doi:10.1126/science.aal4108, 2017.

Anjali, H., Muhammad, A., Anthony, D. M., Karen, S., R., S. M., Mick, M., M., T. A., J., A.
M. and Martine, D.: Impact of Fine Particulate Matter ($PM_{2.5}$) Exposure During Wildfires on
Cardiovascular Health Outcomes, J. Am. Heart Assoc., 4(7), e001653,
doi:10.1161/JAHA.114.001653, 2019.

Black, C., Tesfaigzi, Y., Bassein, J. A. and Miller, L. A.: Wildfire smoke exposure and
human health: Significant gaps in research for a growing public health issue, Environ.
Toxicol. Pharmacol., 55, 186–195, doi:https://doi.org/10.1016/j.etap.2017.08.022, 2017.

Brey, S. J., Ruminski, M., Atwood, S. A. and Fischer, E. V: Connecting smoke plumes to

sources using Hazard Mapping System (HMS) smoke and fire location data over North America, Atmos. Chem. Phys., 18(3), 1745–1761, doi:10.5194/acp-18-1745-2018, 2018.

Dempsey, F.: Forest Fire Effects on Air Quality in Ontario: Evaluation of Several Recent Examples, Bull. Am. Meteorol. Soc., 94(7), 1059–1064, doi:10.1175/BAMS-D-11-00202.1, 2013.

Dominici, F., Peng, R. D., Bell, M. L., Pham, L., McDermott, A., Zeger, S. L. and Samet, J. M.: Fine Particulate Air Pollution and Hospital Admission for Cardiovascular and Respiratory Diseases, JAMA, 295(10), 1127–1134, doi:10.1001/jama.295.10.1127, 2006.

Diao, M., Holloway, T., Choi, S., O'Neill, S.M., Al-Hamdan, M.Z., Van Donkelaar, A., Martin, R.V., Jin, X., Fiore, A.M., Henze, D.K. and Lacey, F., 2019. Methods, availability, and applications of PM2. 5 exposure estimates derived from ground measurements, satellite, and atmospheric models. *Journal of the Air & Waste Management Association*, *69*(12), pp.1391-1414.

Ford, B., Val Martin, M., Zelasky, S. E., Fischer, E. V, Anenberg, S. C., Heald, C. L. and Pierce, J. R.: Future Fire Impacts on Smoke Concentrations, Visibility, and Health in the Contiguous United States, GeoHealth, 2(8), 229–247, doi:10.1029/2018GH000144, 2018.

Gillett, N. P., Weaver, A. J., Zwiers, F. W. and Flannigan, M. D.: Detecting the effect of climate change on Canadian forest fires, Geophys. Res. Lett., 31(18), doi:10.1029/2004GL020876, 2004.

Gunsch, M. J., May, N. W., Wen, M., Bottenus, C. L. H., Gardner, D. J., VanReken, T. M., Bertman, S. B., Hopke, P. K., Ault, A. P. and Pratt, K. A.: Ubiquitous influence of wildfire emissions and secondary organic aerosol on summertime atmospheric aerosol in the forested Great Lakes region, Atmos. Chem. Phys., 18(5), 3701–3715, doi:10.5194/acp-18-3701-2018, 2018.

Guan S, Wong DC, Gao Y, Zhang T, Pouliot G. Impact of wildfire on particulate matter in the southeastern United States in November 2016. Sci Total Environ. 2020;724:138354. doi:10.1016/j.scitotenv.2020.138354.

Johnston F. H., Henderson. S. B., Yang, C., T., R. J., Miriam, M., S., D. R., Patrick, K., M.J.S., B. D. and Michael, B.: Estimated Global Mortality Attributable to Smoke from Landscape Fires, Environ. Health Perspect., 120(5), 695–701, doi:10.1289/ehp.1104422, 2012.

Harris, R. M. B., Remenyi, T. A., Williamson, G. J., Bindoff, N. L., and Bowman, D. M. J. S.: Climate-vegetation fire interactions and feedbacks: trivial detail or major barrier to projecting the future of the Earth system?, Wires Clim. Change, 7, 910-931, 10.1002/wcc.428, 2016.

Hantson, S., Arneth, A., Harrison, S. P., Kelley, D. I., Prentice, I. C., Rabin, S. S., et al. (2016). The status and challenge of global fire modelling. Biogeosciences, 13, 3359–3375. https://doi.org/10.5194/bg-13-3359-2016

Hu, X., Yu, C., Tian, D., Ruminski, M., Robertson, K., Waller, L. A. and Liu, Y.: Comparison of the Hazard Mapping System (HMS) fire product to ground-based fire records in Georgia, USA, J. Geophys. Res. Atmos., 121(6), 2901–2910, doi:10.1002/2015JD024448, 2016.

644 HURTT, G. C., FROLKING, S., FEARON, M. G., MOORE, B., SHEVLIAKOVA, E.,
645 MALYSHEV, S., PACALA, S. W. and HOUGHTON, R. A.: The underpinnings of land-use
646 history: three centuries of global gridded land-use transitions, wood-harvest activity, and
647 resulting secondary lands, Glob. Chang. Biol., 12(7), 1208–1229, doi:10.1111/j.1365-
648 2486.2006.01150.x, 2006.

649 Jaffe, D., Hafner, W., Chand, D., Westerling, A. and Spracklen, D.: Interannual Variations in
650 PM$_{2.5}$ due to Wildfires in the Western United States, Environ. Sci. Technol., 42(8), 2812–
651 2818, doi:10.1021/es702755v, 2008.

652 Jolly, W. M., Cochrane, M. A., Freeborn, P. H., Holden, Z. A., Brown, T. J., Williamson, G.
653 J. and Bowman, D. M. J. S.: Climate-induced variations in global wildfire danger from 1979
654 to 2013, Nat. Commun., 6, 7537 [online] Available from:
655 https://doi.org/10.1038/ncomms8537, 2015.

656 Kaulfus, A. S., Nair, U., Jaffe, D., Christopher, S. A. and Goodrick, S.: Biomass Burning
657 Smoke Climatology of the United States: Implications for Particulate Matter Air Quality,
658 Environ. Sci. Technol., 51(20), 11731–11741, doi:10.1021/acs.est.7b03292, 2017.

659 Kirchmeier-Young, M. C., Zwiers, F. W., Gillett, N. P. and Cannon, A. J.: Attributing
660 extreme fire risk in Western Canada to human emissions, Clim. Change, 144(2), 365–379,
661 doi:10.1007/s10584-017-2030-0, 2017.

662 Kitzberger, T., Falk, D. A., Westerling, A. L. and Swetnam, T. W.: Direct and indirect
663 climate controls predict heterogeneous early-mid 21st century wildfire burned area across
664 western and North America, PLoS One, 12(12), e0188486 [online] Available from:
665 https://doi.org/10.1371/journal.pone.0188486, 2017.

666 Knorr, W., Dentener, F., Lamarque, J.-F., Jiang, L. and Arneth, A.: Wildfire air pollution
667 hazard during the 21st century, Atmos. Chem. Phys., 17(14), 9223–9236, doi:10.5194/acp-
668 17-9223-2017, 2017.

669 Koplitz, S.N., Nolte, C.G., Pouliot, G.A., Vukovich, J.M. and Beidler, J., 2018. Influence of
670 uncertainties in burned area estimates on modeled wildland fire PM2. 5 and ozone pollution
671 in the contiguous US. *Atmospheric environment*, *191*, pp.328-339.

672 Lamarque, J. F., Bond, T. C., Eyring, V., Granier, C., Heil, A., Klimont, Z., Lee, D., Liousse,
673 C., Mieville, A., Owen, 628 B., Schultz, M. G., Shindell, D., Smith, S. J., Stehfest, E., Van
674 Aardenne, J., Cooper, O. R., Kainuma, M., 629 Mahowald, N., McConnell, J. R., Naik, V.,
675 Riahi, K., and van Vuuren, D. P.: Historical (1850-2000) gridded anthropogenic and biomass
676 burning emissions of reactive gases and aerosols: methodology and application, 631 Atmos.
677 Chem. Phys., 10, 7017-7039, 10.5194/acp-10-7017-2010, 2010.

678 Leibensperger, E. M., Mickley, L. J., Jacob, D. J., Chen, W.-T., Seinfeld, J. H., Nenes, A.,
679 Adams, P. J., Streets, D. G., Kumar, N. and Rind, D.: Climatic effects of 1950–2050
680 changes in US anthropogenic aerosols – Part 2: Climate response, Atmos. Chem.
681 Phys., 12(7), 3349–3362, doi:10.5194/acp-12-3349-2012, 2012.

682 Li, F., Zeng, X. D., & Levis, S. (2012). A process-based fire parameterization of intermediate
683 complexity in a dynamic global vegetation model. Biogeosciences, 9(7), 2761–2780.
684 https://doi.org/10.5194/bg-9-2761-2012

685 Liu, J. C., Mickley, L. J., Sulprizio, M. P., Dominici, F., Yue, X., Ebisu, K., Anderson, G. B.,
686 Khan, R. F. A., Bravo, M. A. and Bell, M. L.: Particulate Air Pollution from Wildfires in the

Western US under Climate Change, Clim. Change, 138(3), 655–666, doi:10.1007/s10584-016-1762-6, 2016.

Liu, Y., Goodrick, S. and Heilman, W.: Wildland fire emissions, carbon, and climate: Wildfire–climate interactions, For. Ecol. Manage., 317, 80–96, doi:https://doi.org/10.1016/j.foreco.2013.02.020, 2014.

Liu, X., Easter, R. C., Ghan, S. J., Zaveri, R., Rasch, P., Shi, X., Lamarque, J. F., Gettelman, A., Morrison, H., Vitt, F., Conley, A., Park, S., Neale, R., Hannay, C., Ekman, A. M. L., Hess, P., Mahowald, N., Collins, W., Iacono, M. J., Bretherton, C. S., Flanner, M. G., and Mitchell, D.: Toward a minimal representation of aerosols in climate models: description and evaluation in the Community Atmosphere Model CAM5, Geosci. Model Dev., 5, 709- 652 739, 10.5194/gmd-5-709-2012, 2012.

Meng, J., Martin, R.V., Li, C., van Donkelaar, A., Tzompa-Sosa, Z.A., Yue, X., Xu, J.W., Weagle, C.L. and Burnett, R.T., 2019. Source Contributions to Ambient Fine Particulate Matter for Canada. *Environmental science & technology*, *53*(17), pp.10269-10278.

McClure, C. D. and Jaffe, D. A.: US particulate matter air quality improves except in wildfire-prone areas, Proc. Natl. Acad. Sci., 115(31), 7901 LP – 7906, doi:10.1073/pnas.1804353115, 2018.

Neale, R. B., Chen, C. C., Gettelman, A., Lauritzen, P. H., Park, S., Williamson, D. L., Conley, A. J., Garcia, R., Kinnison, D., Lamarque, J. F., Marsh, D., Mills, M., Smith, A. K., Tilmes, S., Vitt, F., Morrison, H., Cameron671 Smith, P., Collins, W. D., Iacono, M. J., Easter, R. C., Ghan, S. J., Liu, X. H., Rasch, P. J., and Taylor, M. A.: Description of the NCAR Community Atmosphere Model (CAM 5.0), NCAR 289, 2013

Nolte, C. G., Spero, T. L., Bowden, J. H., Mallard, M. S. and Dolwick, P. D.: The potential effects of climate change on air quality across the conterminous US at 2030 under three Representative Concentration Pathways, Atmos. Chem. Phys., 18(20), 15471–15489, doi:10.5194/acp-18-15471-2018, 2018.

Katelyn O'Dell, Bonne Ford, Emily V. Fischer, and Jeffrey R. Pierce Environmental Science & Technology 2019 53 (4), 1797-1804, DOI: 10.1021/acs.est.8b05430.

Partain, J. L., Alden, S., Strader, H., Bhatt, U. S., Bieniek, P. A., Brettschneider, B. R., Walsh, J. E., Lader, R. T., Olsson, P. Q., Rupp, T. S., Thoman, R. L., York, A. D. and Ziel, R. H.: An Assessment of the Role of Anthropogenic Climate Change in the Alaska Fire Season of 2015, Bull. Am. Meteorol. Soc., 97(12), S14–S18, doi:10.1175/BAMS-D-16-0149.1, 2016.

Park, S., Bretherton, C. S., and Rasch, P. J.: Integrating Cloud Processes in the Community Atmosphere Model, Version 5, J. Climate, 27, 6821-6856, 10.1175/Jcli-D-14-00087.1, 2014.

Park, R.J., Jacob, D.J. and Logan, J.A., 2007. Fire and biofuel contributions to annual mean aerosol mass concentrations in the United States. *Atmospheric Environment*, *41*(35), pp.7389-7400.

Pierce, J. R., Val Martin, M., & Heald, C. L. (2017). Estimating the Effects of Changing Climate on Fires and Consequences for U.S. Air Quality, Using a Set of Global and Regional Climate Models (final report no. JFSP-13-1-01-4). Retrieved from https://www.firescience.gov/projects/ 13-1-01-4/project/13-1-01-4_final_report.pdf

Pouliot G, Pace TG, Roy B, Pierce T, Mobley D. Development of a biomass burning emissions inventory by combining satellite and ground-based information. J Appl Remote Sens. 2008;2:021501. doi: 10.1117/1.2939551.

Randerson, J. T., Chen, Y., van der Werf, G. R., Rogers, B. M., & Morton, D. C. (2012). Global burned area and biomass burning emissions from small fires. Journal of Geophysical Research, 117, G04012. https://doi.org/10.1029/2012JG002128

Rolph, G. D., Draxler, R. R., Stein, A. F., Taylor, A., Ruminski, M. G., Kondragunta, S., Zeng, J., Huang, H.-C., Manikin, G., McQueen, J. T. and Davidson, P. M.: Description and Verification of the NOAA Smoke Forecasting System: The 2007 Fire Season, Weather Forecast., 24(2), 361–378, doi:10.1175/2008WAF2222165.1, 2009.

Spracklen, D. V., Mickley, L. J., Logan, J. A., Hudman, R. C., Yevich, R., Flannigan, M. D., & Westerling, A. L. (2009). Impacts of climate change from 2000 to 2050 on wildfire activity and carbonaceous aerosol concentrations in the western United States. Journal of Geophysical Research, 114, D20301. https://doi.org/10.1029/2008JD010966

Sun, Y., Gu, L. H., and Dickinson, R. E.: A numerical issue in calculating the coupled carbon and water fluxes in a climate model, J. Geophys. Res.-Atmos., 117, D2210310.1029/2012jd018059, 2012

Sofiev, M., Ermakova, T., and Vankevich, R.: Evaluation of the smoke-injection height from wild-land fires using remote-sensing data, Atmos. Chem. Phys., 12, 1995-2006, 10.5194/acp-12-1995-2012, 2012

Shi, H., Jiang, Z., Zhao, B., Li, Z., Chen, Y., Gu, Y., Jiang, J. H., Lee, M., Liou, K.-N., Neu, J. L., Payne, V. H., Su, H., Wang, Y., Witek, M. and Worden, J.: Modeling Study of the Air Quality Impact of Record-Breaking Southern California Wildfires in December 2017, J. Geophys. Res. Atmos., 0(0), doi:10.1029/2019JD030472, 2019.

U.S. EPA (U.S. Environmental Protection Agency). 2009. Integrated Science Assessment (ISA) For Particulate Matter (Final Report). EPA/600/R-08/139F.Washington, DC:U.S. EPA.

U.S. EPA. 2018. Our Nation's Air. https://gispub.epa.gov/air/trendsreport/2018/

Val Martin, M., Heald, C. L., Lamarque, J.-F., Tilmes, S., Emmons, L. K. and Schichtel, B. A.: How emissions, climate, and land use change will impact mid-century air quality over the United States: a focus on effects at national parks, Atmos. Chem. Phys., 15(5), 2805–2823, doi:10.5194/acp-15-2805-2015, 2015.

Van der Werf, G. R., Randerson, J. T., Giglio, L., Collatz, G. J., Kasibhatla, P. S., and Arellano, A. F.: Interannual variability in global biomass burning emissions from 1997 to 2004, Atmos. Chem. Phys., 6, 3423-3441, DOI 737 10.5194/acp-6-3423-2006, 2006

Van Der Werf, G. R., Randerson, J. T., Giglio, L., Collatz, G. J., Mu, M., Kasibhatla, P. S., Morton, D. C., Defries, R. S., Jin, Y. and Van Leeuwen, T. T.: Global fire emissions and the contribution of deforestation, savanna, forest, agricultural, and peat fires (1997-2009), Atmos. Chem. Phys., 10(23), 11707–11735, doi:10.5194/acp-10-11707-2010, 2010.

Van Donkelaar, A., R. V. Martin, M. Brauer, N. C. Hsu, R. A. Kahn, R. C. Levy, A. Lyapustin, A. M. Sayer, and D. M. Winker. 2018. Global Annual $PM_{2.5}$ Grids from MODIS, MISR and SeaWiFS Aerosol Optical Depth (AOD) with GWR, 1998-2016. Palisades NY:

771   NASA Socioeconomic Data and Applications Center (SEDAC).
772   https://doi.org/10.7927/H4ZK5DQS. Accessed 16 November 2019.

773   Ward, D. S., Kloster, S., Mahowald, N. M., Rogers, B. M., Randerson, J. T. and Hess, P. G.:
774   The changing radiative forcing of fires: global model estimates for past, present and future,
775   Atmos. Chem. Phys., 12(22), 10857–10886, doi:10.5194/acp-12-10857-2012, 2012.

776   Wotton, B. M., Flannigan, M. D., and Marshall, G. A.: Potential climate change impacts on
777   fire intensity and key wildfire suppression thresholds in Canada, Environ. Res. Lett., 12,
778   095003, https://doi.org/10.1088/1748-9326/aa7e6e, 2017.

779   Westerling, A. L., Hidalgo, H. G., Cayan, D. R. and Swetnam, T. W.: Warming and Earlier
780   Spring Increase Western U.S. Forest Wildfire Activity, Science (80-.)., 313(5789), 940 LP –
781   943, doi:10.1126/science.1128834, 2006.

782   Wotawa, G. and Trainer, M.: The Influence of Canadian Forest Fires on Pollutant
783   Concentrations in the United States, Science (80-.)., 288(5464), 324 LP – 328,
784   doi:10.1126/science.288.5464.324, 2000.

785   Wu, Y., Arapi, A., Huang, J., Gross, B. and Moshary, F.: Intra-continental wildfire smoke
786   transport and impact on local air quality observed by ground-based and satellite remote
787   sensing in New York City, Atmos. Environ., 187, 266–281,
788   doi:https://doi.org/10.1016/j.atmosenv.2018.06.006, 2018.

789   Xue, Z., Gupta, P., and Christopher, S.: Satellite-based estimation of the impacts of
790   summertime wildfires on PM2.5concentration in the United States, Atmos. Chem. Phys., 21,
791   11243–11256, https://doi.org/10.5194/acp-21-11243-2021, 2021.

792   Yang, P.-L., Y. Zhang, K. Wang, P. Doraiswamy, and S.-H. Cho, 2019, Health Impacts and
793   Cost-Benefit Analyses of Surface O_3 and $PM_{2.5}$ over the U.S. under Future Climate and
794   Emission Scenarios, *Environmental Research*, 178, November 2019, 108687,
795   https://doi.org/10.1016/j.envres.2019.108687.

796   Yue, X., Mickley, L. J., Logan, J. A. and Kaplan, J. O.: Ensemble projections of wildfire
797   activity and carbonaceous aerosol concentrations over the western United States in the mid-
798   21st century, Atmos. Environ., 77, 767–780,
799   doi:https://doi.org/10.1016/j.atmosenv.2013.06.003, 2013.

800   Zou, Y., Wang, Y., Ke, Z., Tian, H., Yang, J. and Liu, Y.: Development of a REgion-Specific
801   Ecosystem Feedback Fire (RESFire) Model in the Community Earth System Model, J. Adv.
802   Model. Earth Syst., 11(2), 417–445, doi:10.1029/2018MS001368, 2019.

803   Zou, Y., Wang, Y., Qian, Y., Tian, H., Yang, J. and Alvarado, E.: Using CESM-RESFire to
804   understand climate–fire–ecosystem interactions and the implications for decadal climate
805   variability, Atmos. Chem. Phys., 20, 995–1020, https://doi.org/10.5194/acp-20-995-2020,
806   2020.

807   Zhang, Y., P.-L. Yang, Y. Gao, R. L. Leung, and M. Bell, 2020, Health and Economic
808   Impacts of Air Pollution Induced by Climate Extremes over the Continental U.S.,
809   *Environmental International*, 143, 105921, https://doi.org/10.1016/j.envint.2020.105921.

810

811